

Corrosion Behavior of Polypyrrole/Mesoporous Silica Nanocontainers Coatings on the Mild Steel

M. Yeganeh*, M. Saremi

School of Metallurgy and Materials Engineering, University College of Engineering, University of Tehran, Tehran, I. R. Iran

(*) Corresponding author: myegane@ut.ac.ir

(Received: 01 Dec. 2013 and accepted: 12 Jan. 2014)

Abstract:

The idea of smart corrosion inhibition is based on either inhibitor consumption where it is needed or reducing harmful matrix interaction with it. In addition, applying corrosion inhibitor in a coating causes many problems such as loss of inhibition capability, coating degradation, or both. A useful technique to overcome this problem is applying of inert host systems of nanometer dimensions as nanocontainers, which is loaded by corrosion inhibitors. In this research, Mesoporous silica nanocontainer powders were applied as corrosion inhibitor hosts. Then, these powders were dispersed in the polypyrrole matrix and the release and protection properties of these composite coatings with and without inhibitor were studied in 0.03 M NaCl. Results showed that in higher pHs and chloride media, the release content of corrosion inhibitor is higher. The substrates were protected in the presence of corrosion inhibitor release from mesoporous silica in the chloride media compared to the coatings without inhibitor.

Keywords: Mesoporous silica, Corrosion inhibitor, Polypyrrole, EIS.

1. INTRODUCTION

A lot of metals and alloys are susceptible to corrosion damage. A conventional technique to improve their corrosion resistance is polymer coating. There is a growing encouragement on developing conducting polymer to improve corrosion resistance as polymer coatings [1-5]. Polypyrrole (Ppy), which is a conductive polymer, has been extensively investigated because of its high conductivity and environmental stability as well as its corrosion behavior [6].

Unfortunately, application of Ppy coatings for corrosion protection of metals and alloys for long times is limited due to its protective anion consuming during redox reactions and surface porosities [7-9]. Ppy coating disadvantages can be minimized by incorporating organic or inorganic

materials embedded within the Ppy structures. The formation of composites with Ppy and ceramic particles such as TiO₂ [10-11], Fe₃O₄ [12-13], clay [8, 14], and ZrO₂ [15] has been reported to improve the mechanical and corrosion resistance of the coating. In addition, doping by some corrosion inhibitors is a method of improving the corrosion protection of Ppy.

Molybdate ions can be entered into polymer structure and can be migrated to the active sites to prevent corrosion [2, 16-20]. In this research, the applied inorganic material is mesoporous silica, which can also serve as the host for corrosion inhibitors.

In the present study, functionalized mesoporous silica powders were applied as a pH-sensitive nanocontainer in the corrosive media. Molybdate ion corrosion inhibitors were loaded in the

functionalized mesoporous silica. Then, these loaded mesoporous silica powders were dispersed in the polypyrrole coatings. By immersing of polypyrrole/inhibitor loaded mesoporous silica in the corrosive media, it is expected that the corrosion inhibitors are released and hinder the corrosion process. For a judgment about the effectiveness of the inhibitor containing coatings, mesoporous silica without any adsorbed inhibitor was applied in the polypyrrole coatings and the corrosion properties of these coatings were compared.

2. EXPERIMENTAL

Mesoporous silica powders were synthesized by mixing surfactant molecules such as hexadecyltrimethylammonium bromide and a silica precursor (tetraethylorthosilicate) as reported in the literatures [21]. Then, the initial mesoporous silica was functionalized by silane group and finally corrosion inhibitors (Molybdate Sodium) were loaded to the mesoporous silica (MS) structures. The obtained powders denoted as MSInh can be applied as corrosion inhibitor nanocontainer in the coatings. The mesoporous silica micrograph was studied with a transmission electron microscope (TEM Tecnai G2 F30 at 300 kV). The specific surface area, average pore diameter and pore volume were obtained from N_2 adsorption-desorption isotherms (BELSORP mini-II). The measurement of corrosion inhibitor release from MSInh was performed by inductively coupled plasma optical emission spectrometry (ICP-OES) model Varian VISTA-MPX in acidic and alkaline media. Furthermore, zeta potential of powders was measured at these pHs using a Malvern Zetasizer in these pHs.

Pyrrrole (Merck for synthesis) for the electropolymerization was distilled and kept refrigerated in the dark before coating. Electropolymerization was performed on mild steel sheet. A potentiostat/galvanostat (PAR EG&G Model 273A) was used to produce Ppy/MS and Ppy/MSInh coatings by galvanostatic method. The solution composition consists of 0.1 M oxalic acid, 0.1 M pyrrole, and 2000 ppm MS or MSInh.

Corrosion properties of Ppy/MS and MSInh in the constant pH value (pH=8) and 0.03 M NaCl

chloride ions was investigated at various times by electrochemical tests. The electrochemical measurements were carried out in a classical electrochemical cell with a steel sheets coated by Ppy/MS and Ppy/MSInh films.

3. RESULT AND DISCUSSION

Figure 1a presents the FESEM morphology of mesoporous silica, where diameter of each mesoporous silica tube varies from about 50 to 300 nm, while their length was in micrometer range. Also, Figure 1b shows TEM morphology of mesoporous silica with hexagonal pores. The average of diameter pores, which was obtained by TEM, was about 4 nm.

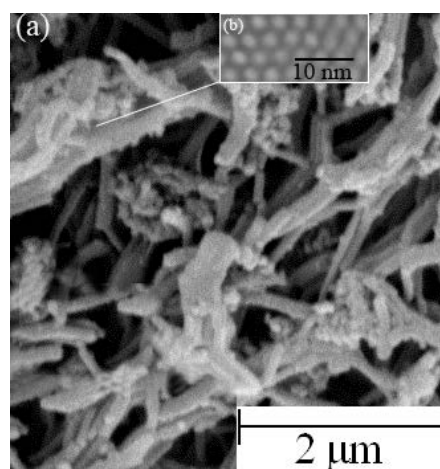


Figure 1: (a) SEM and (b) TEM micrograph of silica mesoporous.

Specific surface area, pore volume and average pore diameter of the mesoporous silica were obtained $776.2 \text{ m}^2 \cdot \text{g}^{-1}$, $0.84 \text{ cm}^3 \cdot \text{g}^{-1}$, and 4.23 nm , respectively by N_2 adsorption/desorption technique. On the other hand, these parameters for MSInh were gained $460.5 \text{ m}^2 \cdot \text{g}^{-1}$, $0.48 \text{ cm}^3 \cdot \text{g}^{-1}$, and 3.1 nm , respectively. Specific surface area, pore volume, and pore diameter size drops after functionalization and adsorption of molybdate ions on the surface of mesoporous silica.

ICP tests showed that molybdate release amount in the alkaline ambient was considerably higher than acidic ambient, which might be due to the surface potential of these powders in the solution [22].

On the other hand, the rate of molybdate release increased with time sharply, and then reached a constant value. Zeta potentials of MSInh powders decreased by increasing pH values from 37.1 to -31.2 mV. This leads to larger electrostatic repulsion forces and faster releases in higher pHs [22]. The MSInh particles at alkaline pHs contain negative charges.

Therefore, it could help electrostatic repulsion forces between the MSInh and molybdate ions and faster release in these ambient. On the other hand, in the acidic ambient, MSInh and molybdate ion have the opposite charge, the attraction between them causes lower release of molybdate ion from MSInh. Thus, applying MSInh nanocontainer in the near neutral and alkaline media is a good approach to make MSInh release in the corrosive ambient.

Figure 2a-b illustrates the open circuit potential (OCP) of Ppy/MS and Ppy/MSInh in 0.03 M NaCl.

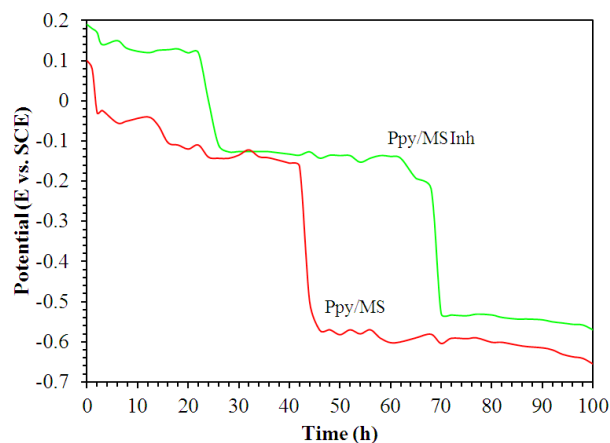


Figure 2: Open circuit potential of (a) Ppy/MS and (b) Ppy/MSInh coating in 0.03 M NaCl

These samples at early stage of immersion are in the positive potential state and this emphasizes that steel coated samples are in the passive state and that thus well protected from corrosive chloride ions [23]. As seen in both Figure 2, at least one distinguished potential plateau was observed for these two coatings. In the case of Ppy/MS, this plateau is similar to passive state of surface in the corrosive media [23].

By passing the time, this plateau disappeared and a sharp decrease in the potential was observed. Finally, the OCP reached the bare steel potential

in the corrosive ion, which is a sign of reaching chloride ion to the steel surface [23]. In the case of Ppy/MSInh coating, the curves have two plateaus. The first plateau is also related to the passivating behavior of polypyrrole in the chloride ion solution. After first breakdown at 22 h, another plateau was observed.

This second plateau is only observed if the incorporated molybdate anion in the polypyrrole can inhibit the corrosion reaction of steel in corrosive media [24]. The molybdate ions can release from MSInh nanocontainers, which are incorporated in the polypyrrole structure. As seen in this figure, the onset of second plateau for Ppy/MSInh is about 26 h.

OCP tests show an increase of the total protection time with the Ppy/MSInh coatings compared to the protection time of the other coatings without inhibitor. The final breakdown time for Ppy/MSInh was recorded 68 h, while the breakdown time for Ppy/MS is about 42 h. It is associated to the release of molybdate ion from MSInh in the corrosive ambient.

Figure 3 shows XRD patterns of steel coated Ppy/MS and Ppy/MSInh after 2 days corrosion in NaCl solution. XRD pattern of steel coated by Ppy/MSInh had the higher Fe peak intensity in comparison with Ppy/MS. Furthermore, the Fe_2O_3 and Fe_3O_4 formed on the steel coated Ppy/MS had the higher intensity and numbers. It shows that the release of molybdate in the steel coated Ppy/MSInh leads to lower corrosion product in chloride media and the surface remains more intact.

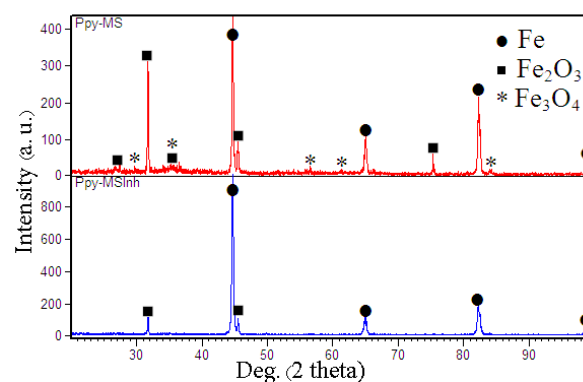


Figure 3: XRD patterns of steel coated Ppy/MS and Ppy/MSInh after 2 days in 0.03 M NaCl solution

Figure 4 demonstrates bode plot of Ppy/MS and MSInh coatings at different times (5 min, 24, 48, and 72 h) in 0.03 M NaCl solution. The optimized values for EIS fitting data obtained from ZView software. Charge transfer resistance of Ppy/MSInh reduced from 1310 to 133 $\Omega\cdot\text{cm}^2$, while this varied from 991 to 61 $\Omega\cdot\text{cm}^2$ for Ppy/MS.

Charge transfer resistances of Ppy/MSInh were higher than Ppy/MS in the early and middle times. This is mainly due to the presence of efficient molybdate ion release in the polypyrrole matrix and the formation of protective compounds on the surface. In the end charge transfer resistance value of both coatings got closer to each other, which was because of lack of any protective layer on the surface, as well as sufficient diffusion of corrosive ions to coatings interfaces.

Also, coating resistance varied from 281 to 60 and 294 to 51 $\Omega\cdot\text{cm}^2$ for Ppy/MSInh and Ppy/MS, respectively. These variations show coating degradation by increasing chloride ion concentration during time. Furthermore, by corrosion process ongoing, the coatings became ion transparent and coating resistance decreased.

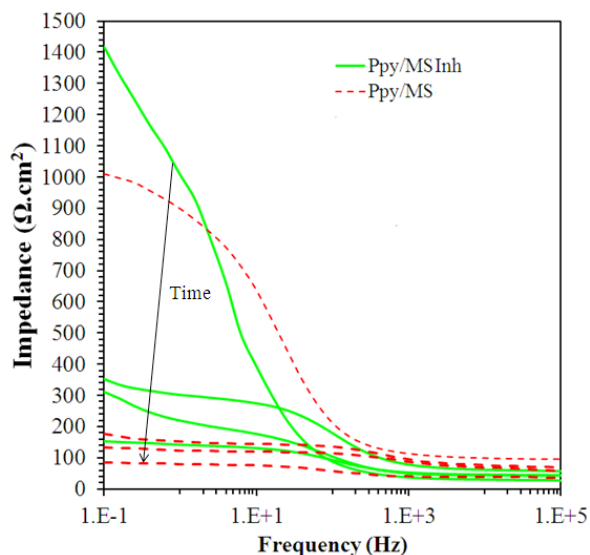


Figure 4: Bode plot of Ppy/MS and Ppy/MSInh coating in $2\text{ g}\cdot\text{dm}^{-3}$ chloride ion solutions at (a) 5 min, (b) 24 h, (c) 48 h, and (d) 72 h.

Figure 5 illustrates Fe ion content within 72 h of immersion, which were released from Ppy/MSInh

and Ppy/MS coatings in chloride ion solutions. The content of Fe ion release from Ppy/MSInh is lower than Ppy/MS at any time. It could be due to higher corrosion resistance of Ppy/MSInh coatings due to molybdate ion release. By reaching 48 h and efficient molybdate release from MSInh, difference of Fe ion release is more obvious. For example, at 6 hours, the difference of Fe ion release from Ppy/MSInh and Ppy/MS was 4 ppm. However, this difference at 48 h reached 70 ppm. This is mainly due to the effect of efficient molybdate release from MSInh in this region.

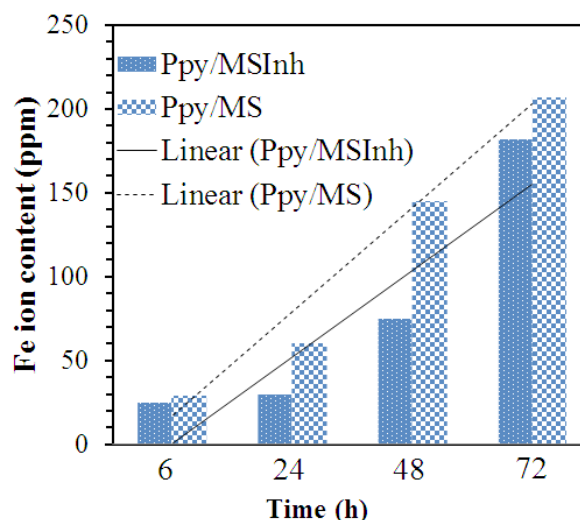


Figure 5: Fe (III) ion content releasing from Ppy/MS and Ppy/MSInh coatings in chloride ion solution and different times.

4. CONCLUSION

In this research, functionalized mesoporous silica loaded by molybdate ion (MSInh) was used as corrosion inhibitor nanocontainer. Then, these powders were incorporated in the polypyrrole substrate to prevent steel corrosion. For comparison, these powders without any inhibitors (MS) were also applied to the polypyrrole coatings.

Results showed that chloride ion concentration caused molybdate ion release because of negative zeta potentials creation on the mesoporous silica. On the other hand release in the alkaline media was easier, due to acidic nature of mesoporous silica. Corrosion studies also revealed that by addition of

MSInh in the coating, surface was more protected than MS one. It was attributed to the formation of protective compounds after release of molybdate in the interface.

5. ACKNOWLEDGMENT

The financial support provided by Chaharmahal and Bakhtiary Province Gas Company is gratefully acknowledged.

REFERENCES

1. W. Su, J. O. Iroh, Synth. Met., Vol. 114., (2000) pp.225-234
2. U. Rammelt, L. M. Duc, W. Plieth, J. Appl. Electrochem., Vol. 35, (2005), pp. 1225-1230.
3. P. Ocon, A.B. Cristobal, P. Herrasti, E. Fatas, Corros. Sci., Vol. 47, (2005), pp.649-662.
4. D. Kowalski, M. Ueda, T. Ohtsuka, Corros. Sci., Vol. 49, (2007), pp. 3442-3452
5. M. Yan, C. A. Vetter, V. J. Gelling, Corros. Sci., Vol. 70, (2013), pp. 37-45
6. B.N. Grgur, N.V. Krstajic', M.V. Vojnovic', C. Lac'njevac, Lj. Gajic'-Krstajic, Prog. Org. Coat., Vol. 33, (1998), pp. 1-6.
7. P. Herrasti, A. N. Kulak, D.V. Bavykin, C. Ponce de Léon, J. Zekonyte, F.C. Walsh, Electrochim. Acta., Vol. 56, (2011), pp. 1323-1328.
8. M. G. Hosseini, M. Raghbi-Boroujeni, I. Ahadzadeh, R. Najjar, M. S. Seyed Dorraji, Prog. Org. Coat., Vol. 66, (2009), pp. 321-327.
9. D. E. Tallman, K. L. Levine, C. Siripirom, V. G. Gelling, G. P. Bierwagen, S. G. Croll, Appl. Surf. Sci., Vol. 254, (2008), pp. 5452-5459.
10. C. A. Ferreira, S. C. Domenech, P. C. Lacaze, J. Appl. Electrochem., Vol. 31, (2001), pp. 49-56.
11. D. M. Lenz, M. Delamar, C. A. Ferreira, J. Electroanal. Chem., Vol. 540, (2003), pp. 35-44
12. B. Garcia, A. Lamzoudi, F. Pillier, H. N. T. Le, C. Deslouis, J. Electrochem. Soc., Vol. 149, (2002), pp. B560- B566.
13. P. Montoya, F. Jaramillo, J. Calderón, S. I. Córdoba de Torresi, R. M. Torresi, Electrochim. Act., Vol. 55, (2010), pp. 6116-6122.
14. J. -M. Yeh, C. -P. Chin, S. Chang, J. Appl. Polym. Sci., Vol. 88, (2003), pp. 3264-3272.
15. A. M. Kumar, N. Rajendran, Surf. Coat. Technol., Vol. 213, (2012), pp. 155-166.
16. I. L. Lehr, S. B. Saidman, Electrochim. Acta , Vol. 51, (2006), pp. 3249- 3255.
17. J. Bonastre, P. Garce's, F. Huerta, C. Quijada, L.G. Andion, F. Cases, Corros. Sci., Vol. 48, (2006), pp. 1122-1136.
18. T. Ohtsuka, M. Iida, M. Ueda, J. Solid State Electrochem., Vol. 10, (2006), pp. 714-720.
19. G. Paliwoda-Porebska, M. Rohwerder, J. Solid State Electrochem., Vol. 10, (2006), pp.730-736
20. M. Mrad, L. Dhouibi, M.F. Montemor, E. Triki, Prog. Org. Coat., Vol. 72, (2011), pp. 511-516.
21. J. S. Beck, et. al.: J. Am. Chem. Soc., Vol. 114, (1992), pp. 10834-10843
22. D. Borisova, H. Mohwald, D. G. Shchukin, ACSNano., Vol. 5, (2011), pp.1939-1946.
23. H. N. T Le, B. Garcia, C. Deslouis, Q. Le Xuan, Electrochim Acta., Vol. 46, (2001), pp. 4259-4272.
24. M. Yan, C. A. Vetter, V. J. Gelling. Corros. Sci., Vol. 70, (2013), pp.37-45.

